Erase, then Redraw: A Novel Data Augmentation Approach for Free Space Detection Using Diffusion Model

Fulong Ma, Weiqing Qi, Guoyang Zhao, Ming Liu, and Jun Ma

Abstract— Data augmentation is one of the most common tools in deep learning, underpinning many recent advances including tasks such as classification, detection, and semantic segmentation. The standard approach to data augmentation involves simple transformations like rotation and flipping to generate new images. However, these new images often lack diversity along the main semantic dimensions within the data. Traditional data augmentation methods cannot alter high-level semantic attributes such as the presence of vehicles, trees, and buildings in a scene to enhance data diversity. In recent years, the rapid development of generative models has injected new vitality into the field of data augmentation. In this paper, we address the lack of diversity in data augmentation for road detection task by using a pre-trained text-to-image diffusion model to parameterize image-to-image transformations. Our method involves editing images using these diffusion models to change their semantics. In essence, we achieve this goal by erasing instances of real objects from the original dataset and generating new instances with similar semantics in the erased regions using the diffusion model (as shown in Fig. 1), thereby expanding the original dataset. We evaluate our approach on the KITTI road dataset [1] and achieve the best results compared to other data augmentation methods, which demonstrates the effectiveness of our proposed development. Here is our project page: https://sites.google.com/view/data-augmentation.
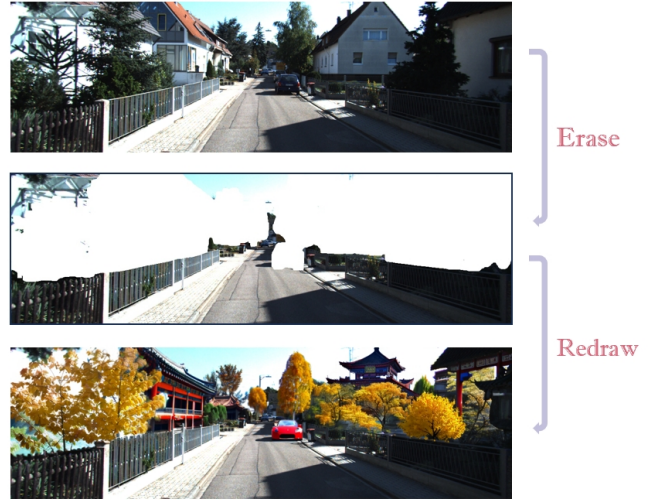
Fig. 1: A schematic diagram of our data augmentation method, it involves first erasing the region of interest within the background of the original image, and then re-drawing within the erased area to generate new synthetic data.

I. INTRODUCTION

In recent years, artificial intelligence has been rapidly advancing, and autonomous driving has emerged as one of the largest engineering applications within the field. It is also considered one of the most challenging areas to develop. For autonomous vehicles, similar to lane detection [2], free space detection is a fundamental component of driving scene understanding. Free space detection methods typically classify each pixel in RGB or depth images as belonging to a drivable area or non-drivable area. These pixel-level classification results are then utilized by other modules in the autonomous driving system, such as trajectory prediction and path planning [3], to ensure that the autonomous vehicle can navigate safely in complex environments [4].

The current mainstream free space detection methods are mainly based on deep learning, which generally require a large amount of manually labeled data to train the algorithms. Manual data labeling is a costly, time-consuming, and labor-intensive task, which greatly affects the practical application of learning-based algorithms. In order to reduce the drawbacks

Fulong Ma, Weiqing Qi, Guoyang Zhao, and Ming Liu are with The Hong Kong University of Science and Technology (Guangzhou), Guangzhou, China. (email: {fmaaf,wqiad,gzhao492}@connect.hkust-gz.edu.cn, eelium@hkust-gz.edu.cn.)

Jun Ma is with The Hong Kong University of Science and Technology (Guangzhou), Guangzhou, China, and also with The Hong Kong University of Science and Technology, Hong Kong SAR, China. (email: jun.ma@ust.hk).

of manual data labeling, researchers have proposed different solutions, including semi-supervised or self-supervised methods. For example, in [5], a semi-supervised learning (SSL) method based on Generative Adversarial Networks (GANs) and a weakly supervised learning (WSL) method based on Conditional GANs (CGANs) was introduced. Compared to semi-supervised methods, self-supervised methods can further reduce the burden of data labeling. Mayr *et al.* [6] proposed a self-supervised method that leverages the v-disparity image to automatically annotate training data for free space. Ma *et al.* [4] utilize depth information from LiDAR combined with road boundary detection to automatically generate training labels for free space on images. In addition to semi-supervised and self-supervised approaches, data augmentation is also an attractive direction. By using various methods to generate more simulated data on a limited training dataset, the original dataset can be expanded to improve the performance of the model.

In this paper, we propose a novel data augmentation method for free space detection. The method is mainly divided into two steps: first, erasing instance pixels in the background using traditional instance segmentation algorithms such as Mask R-CNN [7] or a general segmentation algorithm like Segment Anything (SAM) [8]. Then, the erased regions are locally redrawn using a pre-trained diffusion model to restore the erased parts in the image, as shown in the Fig. 1. During

the redrawing process, different linguistic prompts can be used to achieve redrawing of different objects and styles, providing great flexibility. We then test our proposed method on the KITTI road dataset [1], and the experimental results demonstrate the effectiveness of our approach. Our main contributions are as follows:

- We propose a novel data augmentation method specifically for the task of free space detection, which generates synthetic data through two steps of erasing background instances and redrawing. To the best of our knowledge, this is the first data augmentation method designed specifically for free space detection.
- During the redrawing process, our method can adjust the objects' categories and styles of the redrawn areas through different text prompts. This distinguishes our method from previous data augmentation techniques and greatly enhances the flexibility of data augmentation.
- We conduct comprehensive experiments on the KITTI road dataset, and the results demonstrate that our data augmentation method achieves the best performance in the free space detection task.
- We integrate our data augmentation method into a user-friendly GUI interface, equipped with both automatic and manual augmented data generation functions to facilitate easier use for users.

II. RELATED WORKS

A. Free Space Detection

Free space detection is generally divided into image-based methods, point cloud-based methods, and multimodal methods. In image-based methods, they can be further divided into methods based on the front view and methods based on Bird's Eye View (BEV). In image-based methods, there are methods that detect obstacles in column pixels [9] to obtain free space, as well as methods based on semantic segmentation [10]. In point cloud-based methods, they can be divided into traditional methods and deep learning-based methods. In traditional methods, the free space is usually determined based on the spatial structure information of the point cloud through geometric rules [11]–[14]. Learning-based methods include projecting point clouds onto a spherical surface, converting them into sphere images for use with 2D convolution methods [15], as well as methods that directly take point clouds as input for deep neural networks [16]. To fully utilize the information from multiple sensors, researchers have developed multimodal fusion methods [17]–[19], to improve algorithm performance. PLARD [18] first converts point clouds into ADI images, then inputs the ADI images together with RGB images into a deep neural network for end-to-end learning. SNE-RoadSeg [17] integrates normal information and image information to detect free space, while USNet [19] utilizes RGB images and binocular depth images combined with uncertainty estimation to achieve precise and efficient free space detection.

B. Diffusion Model

The diffusion model is a borrowed concept from thermodynamics, originating from the phenomenon of diffusion. In the field of statistics, this term refers to the process of transforming complex distributions into simpler distributions. In artificial intelligence, the diffusion model [20] defines a probabilistic distribution transformation model, where the forward propagation process can transform a complex distribution into a standard normal distribution. Currently, the diffusion model has achieved significant applications in multiple fields. For image generation task, Stable Diffusion [21] can generate high-quality picture from noise under the guidance of text prompts. This has wide application prospects in areas such as art creation and game design. Text generation [22], By training the diffusion model to learn the distribution of text data, we can generate text content with a certain semantic coherence. This has important application value in natural language processing, machine translation, and other fields. Data augmentation [23], In cases where the dataset is small or the annotation cost is high, we can use the diffusion model for data augmentation, generating more training samples to improve the model's performance.

C. Data Augmentation

Data augmentation aims to generate additional training data through certain methods to enhance model performance, including improving robustness, generalization ability, avoiding overfitting, and so on. Data augmentation can be divided into basic data augmentation and advanced data augmentation. In basic data augmentation methods, there are mainly three types: image manipulation, image erasing, and image mix. Image manipulations focus on image transformations, such as rotation, flipping, and cropping, etc [24]. Image erasing typically deletes one or more sub-regions in the image, with the main idea being to replace the pixel values of these sub-regions with constant values or random values [25]. Image Mix methods are mainly accomplished by mixing two or more images or sub-regions of images into one [26]. In terms of advanced approaches, there are mainly three directions: auto augment, feature augmentation, and deep generative models. Auto augment is based on the fact that different data have different characteristics, so different data augmentation methods have different benefits [27]. Rather than conducting augmentation only in the input space, feature augmentation performs the transformation in a learned feature space [28]. The core idea of deep generative models is that the data distribution we generate data from should not be different from the original one, with GANs [29] being one of the representative methods.

III. METHOD

A. Preliminaries: Diffusion Model

The diffusion probabilistic model was introduced in [30], abbreviated as diffusion model. This is the pioneering work that applied the diffusion model to the field of image generation. Diffusion model is a Markov chain that includes both a forward process with a specific expression, and a
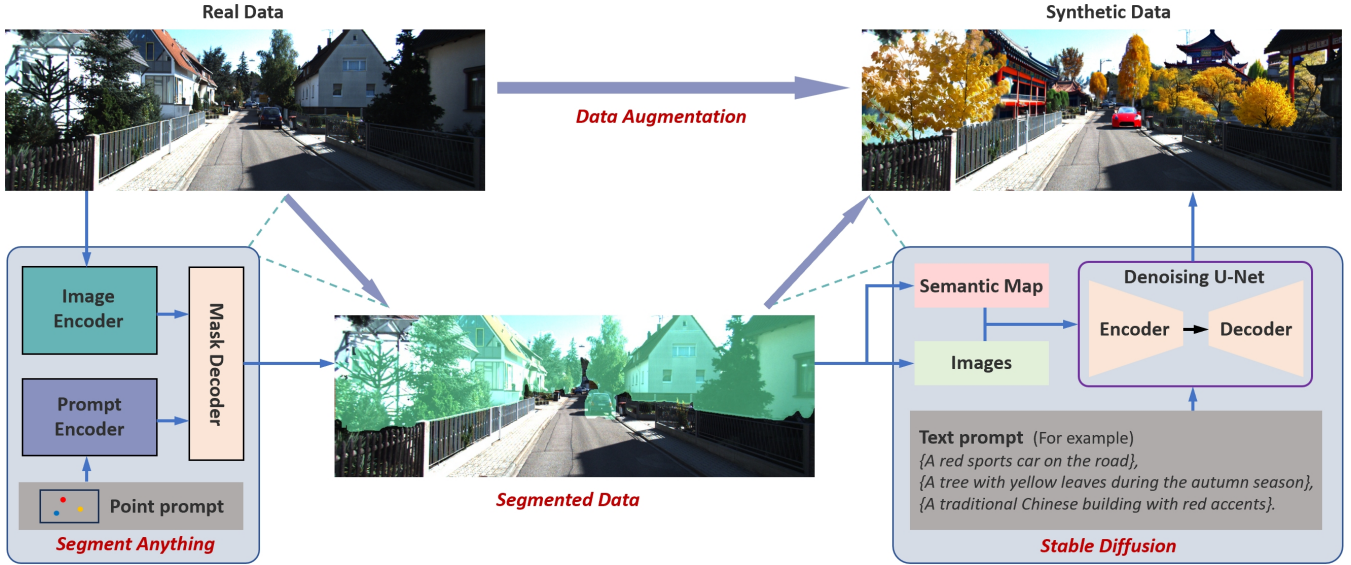
Fig. 2: The architecture of our proposed data augmentation pipeline. Our pipeline consists of two parts, namely, SAM based erasing and stable diffusion based scene redrawing.

backward process that is learned using neural networks. For the forward process, for an image x_0, apply a forward diffusion Markov process to add noise to the image over multiple time steps t with a scheduled variance β_t:

$$q(x_t|x_{t-1}) = \mathcal{N}(x_t; \sqrt{1 - \beta_t}x_t, \beta_t\mathbf{I}), \qquad (1)$$

$$q(x_{1:T}|x_0) = \prod_{t=1}^{T} q(x_t|x_{t-1}), \qquad (2)$$

where T represents the complete set of steps. As T approaches infinity, the resulting output will tend to an pure Gaussian distribution. Through the Markov process, we can calculate x_t by:

$$\begin{aligned} x_t &= \sqrt{\alpha_t}x_{t-1} + \sqrt{1 - \alpha_t}\epsilon_{t-1} \\ &= \sqrt{\bar{\alpha}_t}x_0 + \sqrt{1 - \bar{\alpha}_t}\epsilon, \end{aligned} \qquad (3)$$

where $\alpha_t = 1 - \beta_t$, $\bar{\alpha}_t = \prod_{i=1}^{t} \alpha_i$, $\epsilon_{t-1}, \epsilon \sim \mathcal{N}(0, \mathbf{I})$. The forward process is the process of adding noise, while the reverse process is the denoising process. If we can gradually obtain the reversed distribution $q(x_{t-1}|x_t)$, we can reconstruct the original image distribution x_0 from the Gaussian distribution. It has been demonstrated that if $q(x_t|x_{t-1})$ satisfies a Gaussian distribution and β is small enough, $q(x_{t-1}|x_t)$ remains a Gaussian distribution. However, $q(x_{t-1}|x_t)$ is unknown, so we use a deep neural network p_θ to approximate this distribution:

$$p_\theta(x_{t-1}|x_t) = \mathcal{N}(x_{t-1}; \mu_\theta(x_t, t), \Sigma_\theta(x_t, t)), \qquad (4)$$

where $\mu_\theta(x_t, t) = \frac{1}{\sqrt{\alpha_t}}(x_t - \frac{\beta_t}{\sqrt{1 - \bar{\alpha}_t}}\epsilon_\theta(x_t, t))$. The loss function for training the diffusion model:

$$\mathcal{L} = \left[\mathbb{E}_{t, x_0, \epsilon_t} ||\epsilon_t - \epsilon_\theta(\sqrt{\bar{\alpha}_t}x_0 + \sqrt{1 - \bar{\alpha}_t}\epsilon_t, t)||^2 \right]. \qquad (5)$$

At inference time, we start from a random noise $x_T \sim \mathcal{N}(0, \mathbf{I})$, and then iteratively apply the model ϵ_θ to obtain x_{t-1} from x_t until $t = 0$.

B. Our Approach

In this section, we will introduce our novel "Erase, then Redraw" data augmentation method, and the overall process is shown in Fig. 2.

Most previous work using generative models for data augmentation focuses on classification, where each sample is assigned a label from a finite set of possible classes. While semantic segmentation can be formulated as a classification task in which each pixel is assigned a class, it introduces an additional difficulty, namely that the position of the objects matters. Existing data augmentation methods primarily involve erasing parts of an image and filling them with black pixels or using parts of other images to fill in the erased regions. The result of these methods is that the generated data disrupts the original vision structure. Although this may enhance algorithm performance, the generated data are quite bizarre and would never be encountered in reality.

Fortunately, with the powerful image generation algorithm like diffusion models, we propose to utilize the shape information of objects in the image background and text prompts to generate higher quality synthetic data for data augmentation. An image x to be augmented contains masks $\{m_i\}_{i=1}^{N}$, where N is the number of masks and each masked region $x \oplus m_i$ contains only one object. For each image-mask pair, we also have a corresponding text prompt p_i, like "a sports car on the road".

In the forward process, we select a segmentation mask m_i from the background for image x and its corresponding text prompt p_i. In our setup, $x_0 = x$ and we add noise only to the pixels within the masked area, not to all pixels.

$$\tilde{x}_t = \sqrt{\bar{\alpha}_t}x_0 + \sqrt{1 - \bar{\alpha}_t}\epsilon, \qquad (6)$$

$$x_t = \tilde{x}_t \oplus m + x_0 \oplus (1 - m), \qquad (7)$$

where $\epsilon \sim \mathcal{N}(0, \mathbf{I})$ and t represents the timestep in the forward process, x_t represents the the image where the mask area

is filled with Gaussian noise, as shown in the "*noise image*" of Fig. 3. We then use the x_t and text prompt p_i as input to the diffusion model so it can utilize the input and clear background information to restore the masked area $x_0 \oplus m_i$. The whole process of this procedure is shown in Fig. 3.

For the "erasing" process, *i.e.*, the masks $\{m_i\}_{i=1}^N$ generation step, we utilized SAM [8] model, proposed by Menta AI. As a foundational model for image segmentation, SAM demonstrates strong generalization capabilities and performs well across different data domains. We employ two erasure modes in our study. The first mode is the single-point mode on our GUI, where objects to be erased are manually selected. In the second method, we use the approach proposed in [31], where text prompts specifying the objects to be erased are used to generate candidate points on the original image. These candidate points are then utilized as point prompts for the SAM model to erase the objects in the original image. Both methods are integrated into our GUI interface for the convenience of researchers.

For the "redrawing" process, *i.e.*, the reverse diffusion process, we used the well-trained Stable Diffusion [21] model. Stable Diffusion can generate high-quality realistic simulation data based on text prompts. The input for Stable Diffusion can be text prompts for generating images from text, or it can be an image along with text prompts, used to adapt the input image based on the text prompt. In our proposed method, our input consists of image and text prompts. By using diverse text prompts (a text prompt generator[1] can be used to conveniently generate high-quality text prompts), we are able to generate a wide variety of synthetic data in different styles, making it very flexible and capable of generating more diverse augmentation data. The synthetic data generated by our method is shown in the last row of Fig. 4.
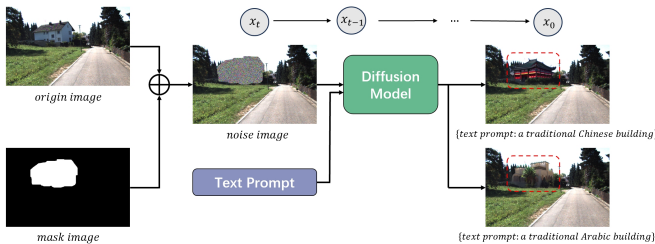

Fig. 3: The redrawing process of our method. After erasing the pixels of the region of interest, new data is generated through the reverse diffusion process of the well-trained diffusion model. Different text prompts can generate new image with different distributions. For example, in the figure, our textual prompts are "*a traditional Chinese building*" and "*a traditional Arabic building*", resulting in the erased area producing buildings with completely different architectural styles.

IV. EXPERIMENT

A. Baselines

In our experiments, we use the following data augmentation methods for comparative experiments: Standard, Basic, RandomErasing [32], Cutout [33], Cutmix [34], and Gridmask

---

TABLE I: Description of baseline methods.

Methods	Description
Standard	No data augmentation is applied, with the algorithm being trained solely on the original dataset provided.
Basic	Dataset undergoes a sequence of transformations, including horizontal flipping, random rotation, brightness and contrast adjustments, and elastic deformation.
RandomErasing	Randomly selects a rectangle region in an image and erases its pixels with random values.
Cutout	Cutout employs a fixed-size square area, filled entirely with 0 (black), and permits the square area to extend outside the image.
CutMix	Randomly select two images, and randomly crop a rectangular area from each image. Then, exchange the cropped areas between the two images and merge them into a new image.
GridMask	Generate a structured grid array first, and then erase the image information within the grid cells.

[34]. Standard represents no data augmentation, where the algorithm is solely trained with the provided dataset, which is randomly split into training and validation sets. Basic represents data augmentation by using the Albumentations library [24], which is also the simplest, most basic, and most commonly used data augmentation method. The visualization of these data augmentation methods are shown in Fig. 4. Similar to our method, DA-Fusion [23] also employs diffusion model to generate simulated data. However, DA-Fusion is specifically designed for classification tasks, it is unsuitable for segmentation tasks. Therefore it is not included in the comparison scope. A summary of all baselines is presented in Table I. The augmented data generated using these methods and our approach is depicted in Fig. 4.

B. Dataset

In our experiments, we used the publicly available KITTI road dataset [1] to validate the effectiveness of our algorithm. The KITTI road dataset is one of the most popular and widely used datasets for road scene understanding and is commonly utilized for tasks such as free space detection and lane line detection, it contains 289 frames training data and 290 frames testing data. When using the KITTI road dataset, it is often necessary to divide the dataset into three parts: training dataset, testing dataset, and validation dataset. However, the official KITTI road dataset only provides the training and testing portions and does not include a validation set. Therefore, researchers need to perform their own partitioning of the training and validation sets. Our data division is as follows: First, we randomly split the training data from the KITTI road dataset into two parts, 144 and 145 images, respectively. Out of these, 144 images are used as the testing dataset. Then, from the 145 images, we randomly select 20% of the data, which amounts to 29 images, as the validation dataset, the remaining 116 images are used as the training dataset.

C. Experiment Setup

Our experiments are conducted in an Ubuntu 20.04 environment, equipped with an Intel i7 12700F CPU and a NVIDIA GeForce RTX 4090 GPU. We employed the PyTorch framework for model training and set training parameters

TABLE II: The experimental results of our data augmentation method, along with other data augmentation methods such as Basic [24], RandomErasing [32], Cutout [33], CutMix [34], and GridMask [25]. To ensure comprehensive experimentation, experiments were conducted on three different classic model on three different network architectures. Bold indicates the best result, while underline indicates the second-best result.

Network	Network Architecture	Augmentation Method	Accuracy	Precision	Recall	F1-Score	mIoU
U-Net [35]	CNN	Standard	94.78	82.74	87.50	85.05	75.42
		Basic	95.19	85.77	87.63	86.70	76.52
		RandomErasing	94.61	79.43	94.23	86.20	75.75
		Cutout	95.76	88.76	87.34	88.05	78.65
		CutMix	95.50	85.94	89.45	87.66	78.04
		GridMask	91.89	69.73	96.50	80.96	68.02
		Ours	**96.59**	**92.42**	88.14	**90.23**	**82.20**
Swin-UNet [36]	Transformer	Standard	93.52	80.60	83.93	82.23	69.83
		Basic	94.76	84.35	86.98	85.59	74.82
		RandomErasing	95.18	84.41	87.98	86.15	77.08
		Cutout	95.25	83.36	88.90	86.04	77.65
		CutMix	95.20	84.51	89.59	86.97	76.96
		GridMask	95.27	**85.72**	88.27	86.98	76.96
		Ours	**95.54**	85.66	**90.16**	**87.85**	**78.34**
VM-UNet [37]	Mamba	Standard	97.86	93.51	94.56	94.03	88.73
		Basic	97.86	92.82	95.39	94.09	88.84
		RandomErasing	98.44	96.14	95.07	95.60	91.58
		Cutout	98.59	**96.99**	95.08	96.03	92.35
		CutMix	98.43	95.60	95.61	95.60	91.57
		GridMask	97.61	93.12	93.51	93.32	87.47
		Ours	**98.65**	96.21	**96.23**	**96.22**	**92.72**

Fig. 4: The comparison between the synthetic data generated by our method and the synthetic data generated by other data augmentation methods. The first row of images represents the original data from the KITTI road dataset [1]. The 2nd, 3rd, 4th, 5th, and 6th rows correspond to the synthetic data generated by the data augmentation methods RandomErasing [32], Cutout [33], Gridmask [25], CutMix [34], and our method, respectively.

with a batch size of 2, a total of 300 epochs. Regarding to the augmented data, we used each data augmentation method to generate 3 synthetic images for each origin image in the KITTI road dataset for training. In the standard experimental setup without any data augmentation, we duplicated each original image three times to maintain fairness in the amount of training data.

D. Evaluation Metrics

Consistent with other free space detection works, we selected five commonly used evaluation metrics to assess the performance of our proposed method. These evaluation metrics are: $Accuracy$, $Precision$, $Recall$, F_{Score} and IoU (intersection over union), and they were computed as follows: $Accuracy = \frac{N_{TP}+N_{TN}}{N_{TP}+N_{FP}+N_{TN}+N_{FN}}, Precision = \frac{N_{TP}}{N_{TP}+N_{FP}}, Recall =$

TABLE III: The experimental results of our data augmentation method, along with other data augmentation methods such as Basic [24], RandomErasing [32], Cutout [33], CutMix [34], and GridMask [25] on two different multi-modal models. Bold indicates the best result, while underline indicates the second-best result.

Network	Network Input	Augmentation Method	Accuracy	Precision	Recall	F1-Score	mIoU
PLARD [18]	RGB + LiDAR	Standard	95.61	92.08	91.09	91.58	85.12
		Basic	97.05	94.15	93.13	93.64	88.20
		RandomErasing	97.87	93.96	93.95	93.96	88.61
		Cutout	97.93	94.40	93.99	94.19	89.03
		CutMix	98.00	94.51	**94.28**	94.40	89.40
		GridMask	97.92	94.81	93.51	94.16	88.96
		Ours	**98.15**	**95.49**	94.11	**94.80**	**90.11**
SNE-RoadSeg [17]	RGB + Depth	Standard	95.97	92.37	91.88	92.12	86.12
		Basic	97.95	94.19	94.37	94.28	89.19
		RandomErasing	98.41	95.81	95.63	95.72	91.79
		Cutout	98.44	95.48	95.84	95.66	91.68
		CutMix	98.30	95.16	95.86	95.51	91.40
		GridMask	98.35	94.90	**95.92**	95.41	91.22
		Ours	**98.66**	**96.89**	95.54	**96.21**	**92.70**

$\frac{N_{TP}}{N_{TP}+N_{FN}}, F1 - Score = \frac{2*Precision*Recall}{Precision+Recall}, IoU = \frac{N_{TP}}{N_{TP}+N_{FP}+N_{FN}}$, where N_{TP}, N_{TN}, N_{FP} and N_{FN} represents the true positive, true negative, false positive, and false negative pixel numbers, respectively.

E. Performance Evaluation

The quantitative experimental results on three different architectures of single-modal algorithms U-Net, Swin-UNet, and VM-UNet are shown in Table II. From the table, it can be seen that our data augmentation method achieves the best performance on three different deep neural network architectures: CNN, Transformer, and Mamba. Specifically, compared to the second best method, on U-Net, our data augmentation method increased the F1-Score from 88.05 to 90.23 and mIoU from 78.65 to 82.20. On Swin-Net, our data augmentation method increased the F1-Score from 86.98 to 87.85 and mIoU from 77.65 to 78.34. On VM-UNet, our data augmentation method improved the F1-Score from 96.03 to 96.22 and mIoU from 92.35 to 92.72. When compared to the Basic method, the F1-Score and mIoU increased by 2.26% and 8.87% on Unet, the F1-Score and mIoU increased by 2.64% and 4.71% on Swin-Unet, and the F1-Score and mIoU increased by 2.05% and 3.94% on VM-Unet.

The quantitative experimental results on two multi-modal algorithms PLARD and SNE-RoadSeg are shown in Table III. From the table, it can be seen that our data augmentation method also achieves the best performance on multi-modal models with different data inputs. Specifically, compared to the second best method, on PLARD, our data augmentation method increased the F1-Score from 94.40 to 94.80 and mIoU from 89.40 to 90.11. On SNE-RoadSeg, our data augmentation method increased the F1-Score from 95.72 to 96.21 and mIoU from 91.79 to 92.70. On PLARD, the F1-Score and mIoU increased by 1.24% and 2.17%, on SNE-RoadSeg, the F1-Score and mIoU increased by 2.05% and 3.94%, respectively.

Based on the experiments conducted on both single-modal and multi-modal algorithms mentioned above, our data

augmentation methods have shown significant improvements, demonstrating the effectiveness of our approach.

V. CONCLUSIONS

In this paper, we propose a novel data augmentation method for free space detection task using SAM model and diffusion models. Our method consists of two steps. First, we utilize a SAM to erase elements from the original data and retain pixel regions belonging to free space. Second, we deploy a pretrained diffusion model to inpaint the erased regions, allowing us to generate diverse and personalized synthetic data by leveraging language prompts. We tested our method on the KITTI road dataset, and the results demonstrate that our data augmentation approach achieves leading performance compared to existing methods. However, our method has a few limitations, and there are several directions for future work. Firstly, our method does not explicitly control how the diffusion model enhances images. Introducing a control mechanism, like the idea of ControlNet [38], in future work could better manage the generation of images in erased regions, potentially improving results. Secondly, expanding the data augmentation method presented in this paper to more vision tasks to enhance its versatility is also a direction worth exploring.

REFERENCES

[1] J. Fritsch, T. Kuehnl, and A. Geiger, "A new performance measure and evaluation benchmark for road detection algorithms," in *IEEE Conference on Intelligent Transportation Systems*, 2013, pp. 1693–1700.

[2] F. Ma, W. Qi, G. Zhao, L. Zheng, S. Wang, and M. Liu, "Monocular 3D lane detection for autonomous driving: Recent achievements, challenges, and outlooks," *arXiv preprint arXiv:2404.06860*, 2024.

[3] J. Thoma, D. P. Paudel, A. Chhatkuli, T. Probst, and L. V. Gool, "Mapping, localization and path planning for image-based navigation using visual features and map," in *Proceedings of the IEEE/CVF Conference on Computer Vision and Pattern Recognition*, 2019, pp. 7383–7391.

[4] F. Ma, Y. Liu, S. Wang, J. Wu, W. Qi, and M. Liu, "Self-supervised drivable area segmentation using LiDAR's depth information for autonomous driving," in *IEEE/RSJ International Conference on Intelligent Robots and Systems*, 2023, pp. 41–48.

[5] X. Han, J. Lu, C. Zhao, S. You, and H. Li, "Semisupervised and weakly supervised road detection based on generative adversarial networks," *IEEE Signal Processing Letters*, vol. 25, no. 4, pp. 551–555, 2018.

[6] J. Mayr, C. Unger, and F. Tombari, "Self-supervised learning of the drivable area for autonomous vehicles," in *IEEE/RSJ International Conference on Intelligent Robots and Systems*, 2018, pp. 362–369.

[7] K. He, G. Gkioxari, P. Dollár, and R. Girshick, "Mask R-CNN," in *Proceedings of the IEEE International Conference on Computer Vision*, 2017, pp. 2961–2969.

[8] A. Kirillov, E. Mintun, N. Ravi, *et al.*, "Segment anything," in *Proceedings of the IEEE/CVF International Conference on Computer Vision*, 2023, pp. 4015–4026.

[9] D. Levi, N. Garnett, E. Fetaya, and I. Herzlyia, "StixelNet: A deep convolutional network for obstacle detection and road segmentation.," in *British Machine Vision Conference*, vol. 1, 2015, p. 4.

[10] X. Liu and Z. Deng, "Segmentation of drivable road using deep fully convolutional residual network with pyramid pooling," *Cognitive Computation*, vol. 10, pp. 272–281, 2018.

[11] P. Narksri, E. Takeuchi, Y. Ninomiya, Y. Morales, N. Akai, and N. Kawaguchi, "A slope-robust cascaded ground segmentation in 3D point cloud for autonomous vehicles," in *International Conference on Intelligent Transportation Systems*, 2018, pp. 497–504.

[12] D. Zermas, I. Izzat, and N. Papanikolopoulos, "Fast segmentation of 3D point clouds: A paradigm on LiDAR data for autonomous vehicle applications," in *IEEE International Conference on Robotics and Automation*, 2017, pp. 5067–5073.

[13] M. Himmelsbach, F. V. Hundelshausen, and H.-J. Wuensche, "Fast segmentation of 3D point clouds for ground vehicles," in *IEEE Intelligent Vehicles Symposium*, 2010, pp. 560–565.

[14] S. Lee, H. Lim, and H. Myung, "Patchwork++: Fast and robust ground segmentation solving partial under-segmentation using 3D point cloud," in *IEEE/RSJ International Conference on Intelligent Robots and Systems*, 2022, pp. 13 276–13 283.

[15] B. Wu, X. Zhou, S. Zhao, X. Yue, and K. Keutzer, "SqueezeSegv2: Improved model structure and unsupervised domain adaptation for road-object segmentation from a lidar point cloud," in *International Conference on Robotics and Automation*, 2019, pp. 4376–4382.

[16] C. R. Qi, H. Su, K. Mo, and L. J. Guibas, "Pointnet: Deep learning on point sets for 3D classification and segmentation," in *Proceedings of the IEEE/CVF Conference on Computer Vision and Pattern Recognition*, 2017, pp. 652–660.

[17] R. Fan, H. Wang, P. Cai, and M. Liu, "SNE-RoadSeg: Incorporating surface normal information into semantic segmentation for accurate freespace detection," in *European Conference on Computer Vision*, 2020, pp. 340–356.

[18] Z. Chen, J. Zhang, and D. Tao, "Progressive LiDAR adaptation for road detection," *IEEE/CAA Journal of Automatica Sinica*, vol. 6, no. 3, pp. 693–702, 2019.

[19] Y. Chang, F. Xue, F. Sheng, W. Liang, and A. Ming, "Fast road segmentation via uncertainty-aware symmetric network," in *International Conference on Robotics and Automation*, 2022, pp. 11 124–11 130.

[20] L. Yang, Z. Zhang, Y. Song, *et al.*, "Diffusion models: A comprehensive survey of methods and applications," *ACM Computing Surveys*, vol. 56, no. 4, pp. 1–39, 2023.

[21] R. Rombach, A. Blattmann, D. Lorenz, P. Esser, and B. Ommer, "High-resolution image synthesis with latent diffusion models," in *Proceedings of the IEEE/CVF Conference on Computer Vision and Pattern Recognition*, 2022, pp. 10 684–10 695.

[22] Y. Li, K. Zhou, W. X. Zhao, and J.-R. Wen, "Diffusion models for non-autoregressive text generation: A survey," *arXiv preprint arXiv:2303.06574*, 2023.

[23] B. Trabucco, K. Doherty, M. Gurinas, and R. Salakhutdinov, "Effective data augmentation with diffusion models," *arXiv preprint arXiv:2302.07944*, 2023.

[24] A. Buslaev, V. I. Iglovikov, E. Khvedchenya, A. Parinov, M. Druzhinin, and A. A. Kalinin, "Albumentations: Fast and flexible image augmentations," *Information*, vol. 11, no. 2, p. 125, 2020.

[25] P. Chen, S. Liu, H. Zhao, and J. Jia, "Gridmask data augmentation," *arXiv preprint arXiv:2001.04086*, 2020.

[26] H. Inoue, "Data augmentation by pairing samples for images classification," *arXiv preprint arXiv:1801.02929*, 2018.

[27] E. D. Cubuk, B. Zoph, D. Mane, V. Vasudevan, and Q. V. Le, "Autoaugment: Learning augmentation strategies from data," in *Proceedings of the IEEE/CVF Conference on Computer Vision and Pattern Recognition*, 2019, pp. 113–123.

[28] T. DeVries and G. W. Taylor, "Dataset augmentation in feature space," *arXiv preprint arXiv:1702.05538*, 2017.

[29] A. Creswell, T. White, V. Dumoulin, K. Arulkumaran, B. Sengupta, and A. A. Bharath, "Generative adversarial networks: An overview," *IEEE Signal Processing Magazine*, vol. 35, no. 1, pp. 53–65, 2018.

[30] J. Ho, A. Jain, and P. Abbeel, "Denoising diffusion probabilistic models," *Advances in Neural Information Processing Systems*, vol. 33, pp. 6840–6851, 2020.

[31] Y. Li, H. Wang, Y. Duan, and X. Li, "Clip surgery for better explainability with enhancement in open-vocabulary tasks," *arXiv preprint arXiv:2304.05653*, 2023.

[32] Z. Zhong, L. Zheng, G. Kang, S. Li, and Y. Yang, "Random erasing data augmentation," in *Proceedings of the AAAI Conference on Artificial Intelligence*, vol. 34, 2020, pp. 13 001–13 008.

[33] T. DeVries and G. W. Taylor, "Improved regularization of convolutional neural networks with cutout," *arXiv preprint arXiv:1708.04552*, 2017.

[34] S. Yun, D. Han, S. J. Oh, S. Chun, J. Choe, and Y. Yoo, "CutMix: Regularization strategy to train strong classifiers with localizable features," in *Proceedings of the IEEE/CVF International Conference on Computer Vision*, 2019, pp. 6023–6032.

[35] O. Ronneberger, P. Fischer, and T. Brox, "U-Net: Convolutional networks for biomedical image segmentation," in *International Conference on Medical Image Computing and Computer-Assisted Intervention*, 2015, pp. 234–241.

[36] H. Cao, Y. Wang, J. Chen, *et al.*, "Swin-Unet: Unet-like pure transformer for medical image segmentation," in *European Conference on Computer Vision*, 2022, pp. 205–218.

[37] J. Ruan and S. Xiang, "VM-Unet: Vision Mamba UNet for medical image segmentation," *arXiv preprint arXiv:2402.02491*, 2024.

[38] L. Zhang, A. Rao, and M. Agrawala, "Adding conditional control to text-to-image diffusion models," in *Proceedings of the IEEE/CVF International Conference on Computer Vision*, 2023, pp. 3836–3847.